Supporting Information

Tunable Ellipsoidal Cage in ZIF-300 and ZIF-301 for Size-Selective Acetone/Butanol Separation

Yanjun Wu,‡ Jiaojiao Song,‡ Jiang Wang and Qi Shi**

College of Chemistry and Chemical Engineering, Taiyuan University of Technology, Taiyuan 030024, P. R. China.

‡Yanjun Wu and Jiaojiao Song contributed equally to this work.

**Corresponding author: Jiang Wang, E-mail: jwang47@163.com; Qi Shi, E-mail: shiqi594@163.com*

Table of Contents

Section S1: Reagent dosage used for synthesizing ZIF-300 and ZIF-301 derivatives.

Table S1. The amount of reagents used for preparing ZIF-300 and ZIF-301 derivatives. The RbIm in the table represent 5-bromo-benzimidazole (bbIm) and 5-chlorobenzimidazole (cbIm), respectively.

Sample	Mole ratio of mIm:RbIm	$Zn(NO_3)_2 \cdot 6H_2O$ (mmol)	mIm (mmol)	RbIm (mmol)
ZIF-300-S1	1.0 : 2.0 : 4.0	3.65	7.30	14.60
ZIF-300-S2	1.0 : 2.0 : 3.0	3.65	7.30	10.95
ZIF-300-S3	1.0 : 2.0 : 2.0	3.65	7.30	7.30
ZIF-300-S4	1.0 : 2.0 : 1.0	3.65	7.30	3.65
ZIF-301-S1	1.0 : 1.0 : 3.0	3.65	3.65	10.95
ZIF-301-S2	1.0 : 1.5 : 3.0	3.65	5.47	10.95
ZIF-301-S3	1.0 : 2.0 : 3.0	3.65	7.30	10.95
ZIF-301-S4	1.0 : 2.0 : 1.0	3.65	7.30	3.65

Section S2: Summary of BET analysis for ZIF-300 and ZIF-301 derivatives.

Table S2. BET summary of ZIF-300 and ZIF-301 derivatives synthesized with varying dual-ligand feeding ratios. The RbIm in the table represent 5-bromo-benzimidazole (bbIm) and 5-chlorobenzimidazole (cbIm), respectively.

Samples	Mole ratio of mIm:RbIm	BET-N_2 (m^2 g^{-1})
ZIF-300	1.0 : 4.0	0.5
	1.0 : 3.0	2.5
	1.0 : 2.0	3
	1.0 : 1.0	230
	2.0 : 4.0	18
	2.0 : 3.0	135
	2.0 : 2.0	301
	2.0 : 1.0	535
ZIF-301	1.0 : 1.0	501
	1.5 : 1.0	537
	2.0 : 1.0	602
	2.5 : 1.0	600
	1.0 : 3.0	25
	1.5 : 3.0	189
	2.0 : 3.0	310
	3.0 : 3.0	547

Section S3: Characterization of ZIF-300 and ZIF-301 derivatives including: PXRD, FT-IR spectra, TG trace, and SEM images.

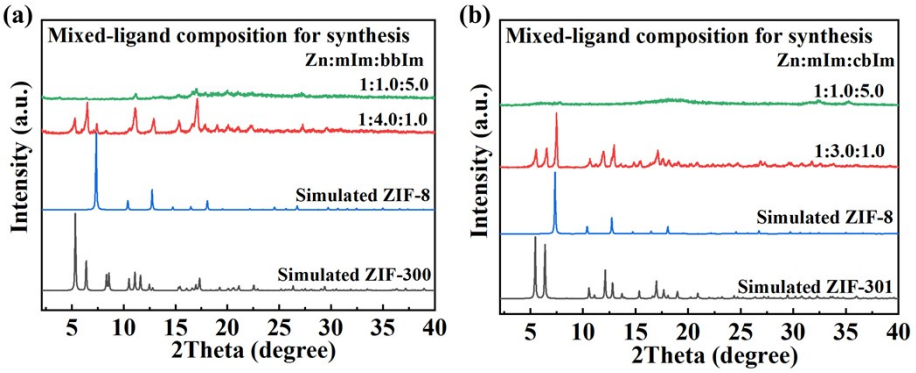

Figure S1 PXRD patterns of the synthesized (a) ZIF-300 and (b) ZIF-301 derivative, and the simulated samples.

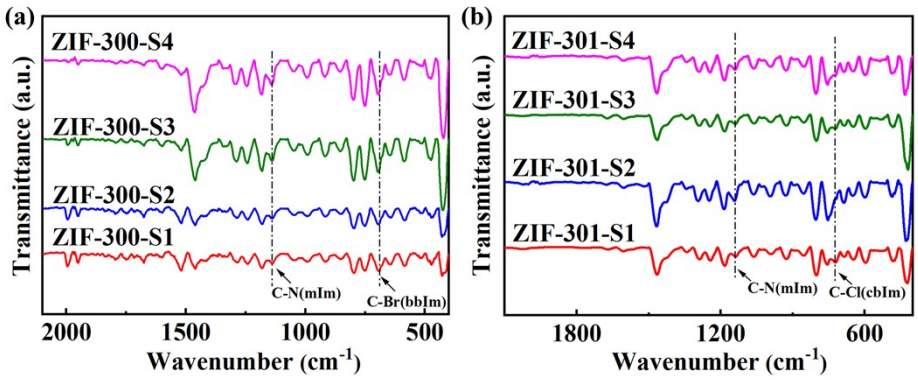

Figure S2 FT-IR spectra of (a) ZIF-300-S1-S4 and (b) ZIF-301-S1-S4

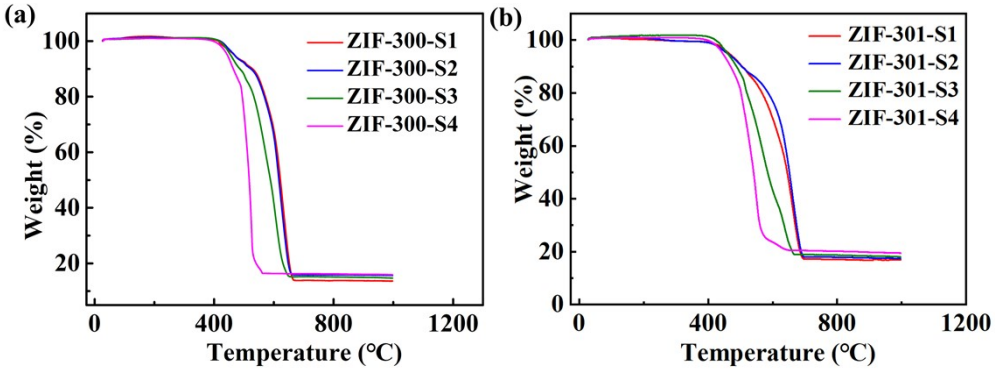

Figure S3 TG curves for (a) ZIF-300-S1-S4 and (b) ZIF-301-S1-S4 at a heating rate of 5 °C min^{-1} under air flow

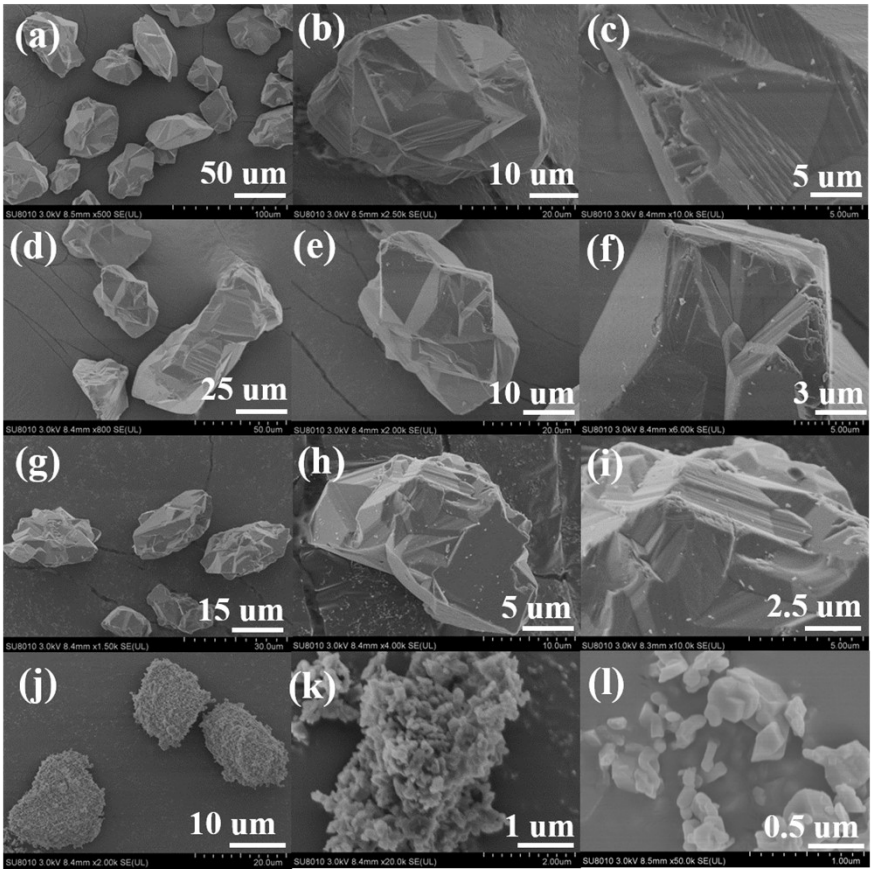

Figure S4 SEM images of the synthetic sample: (a-c) ZIF-300-S1, (d-f) ZIF-300-S2, (g-i) ZIF-300-S3, (j-l) ZIF-300-S4

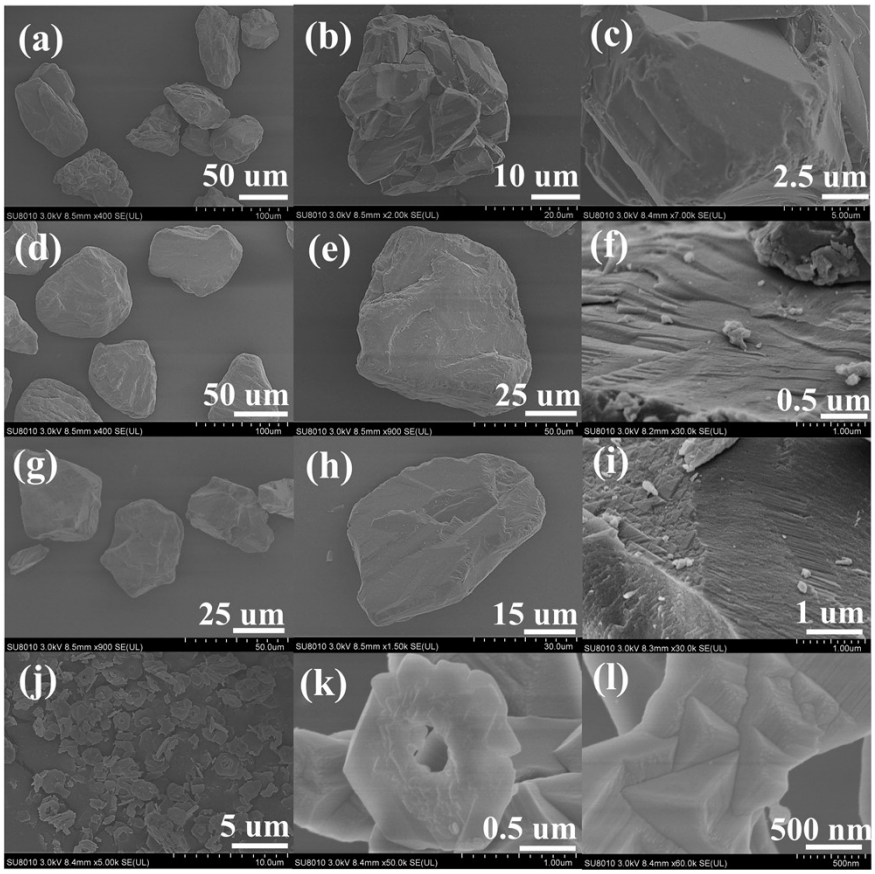

Figure S5 SEM images of the synthetic sample: (a-c) ZIF-301-S1, (d-f) ZIF-301-S2, (g-i) ZIF-301-S3, (j-l) ZIF-301-S4

Section S4: Hydrophobicity of ZIF-300 and ZIF-301 derivatives.

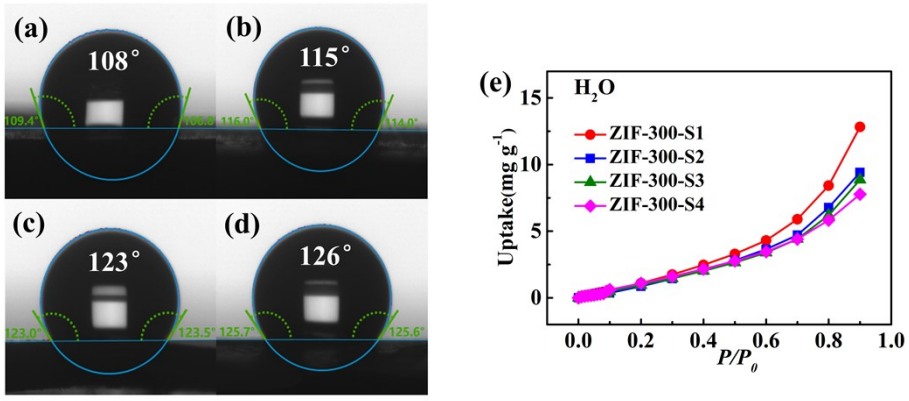

Figure S6 Contact angle measurements for (a-d) ZIF-300-S1-S4. (e) the water vapor adsorption of ZIF-300-S1-S4 at 298 K.

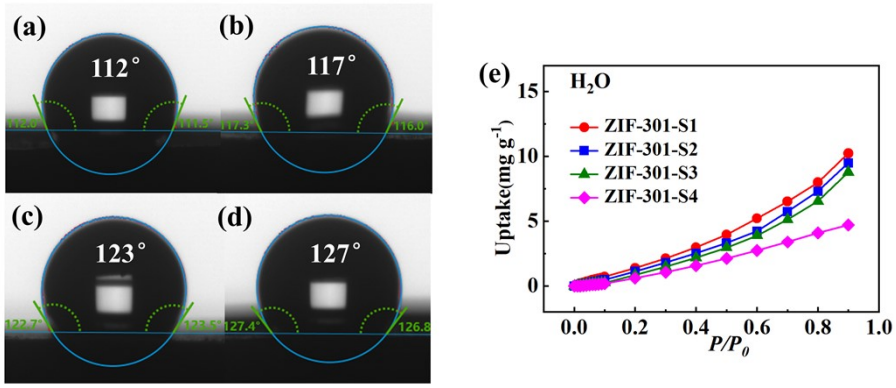

Figure S7 Contact angle measurements for (a-d) ZIF-301-S1-S4, (e) water vapor adsorption of ZIF-301-S1-S4 at 298 K

Section S5: Single component static adsorption isotherms of ZIF-300 and ZIF-301 derivatives for butanol and acetone.

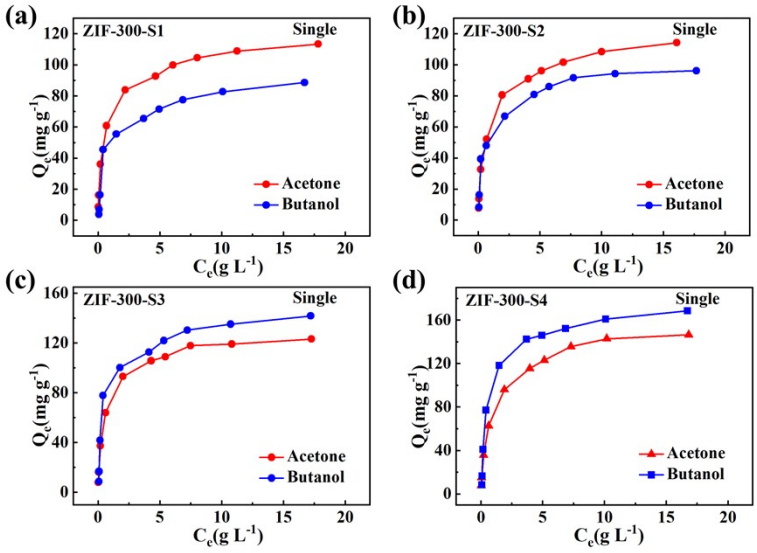

Figure S8 The static adsorption isotherm of (a) ZIF-300-S1, (b) ZIF-300-S2, (c) ZIF-300-S3, and (d) ZIF-300-S4 for single component acetone and butanol at 298 K

Table S3 Static adsorption data of single component butanol and acetone by ZIF-300-S1-S4 at 298 K

Adsorbent	Adsorbate	Static batch adsorption of ABE single component	
		Concentration of stock solution (g L^{-1})	Adsorption amount (mg g^{-1})
ZIF-300-S1	Acetone	20.1	113.1
	Butanol	20.0	88.6
ZIF-300-S2	Acetone	19.7	114.2
	Butanol	19.5	96.1
ZIF-300-S3	Acetone	19.6	123.9
	Butanol	20.0	141.7
ZIF-300-S4	Acetone	19.8	146.4
	Butanol	20.1	168.6

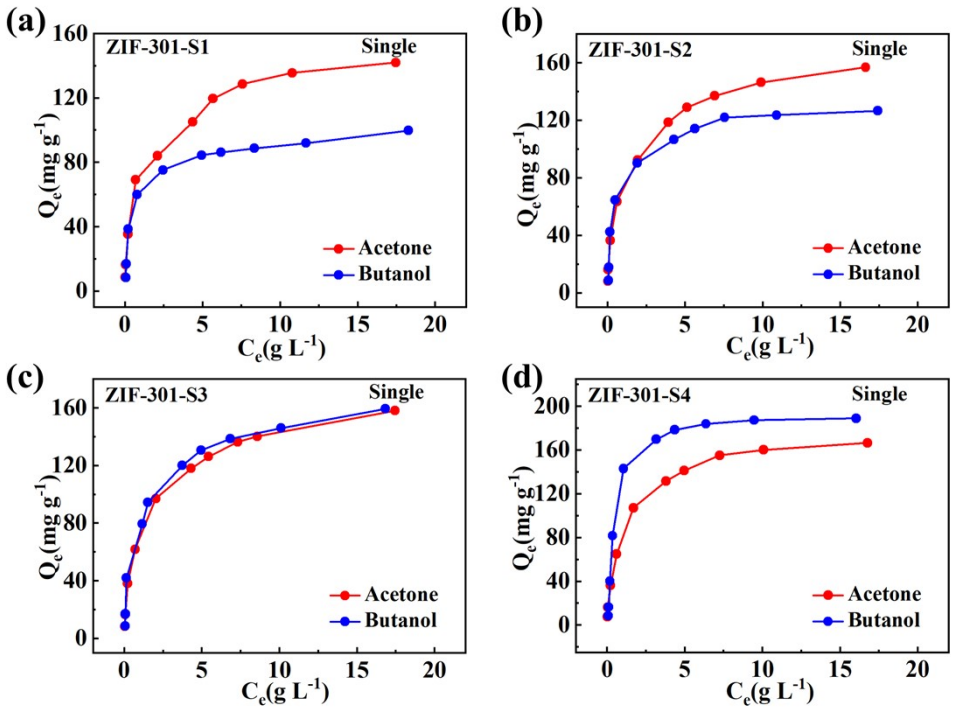

Figure S9 The static adsorption isotherm of (a) ZIF-301-S1, (b) ZIF-301-S2, (c) ZIF-301-S3, and (d) ZIF-301-S4 for single component acetone and butanol at 298 K

Table S4 Static adsorption data of single component butanol and acetone by ZIF-301-S1-S4 at 298 K

Adsorbent	Adsorbate	Static batch adsorption of ABE single component	
		Concentration of stock solution ($g\ L^{-1}$)	Adsorption amount ($mg\ g^{-1}$)
ZIF-301-S1	Acetone	20.3	143.1
	Butanol	20.4	106.2
ZIF-301-S2	Acetone	19.9	156.8
	Butanol	20.0	126.6
ZIF-301-S3	Acetone	20.3	158.2
	Butanol	20.0	159.7
ZIF-301-S4	Acetone	20.0	166.4
	Butanol	19.8	189.5

Section S6: Breakthrough curves, saturated capacity, and selectivity of ZIF-300 and ZIF-301 derivatives.

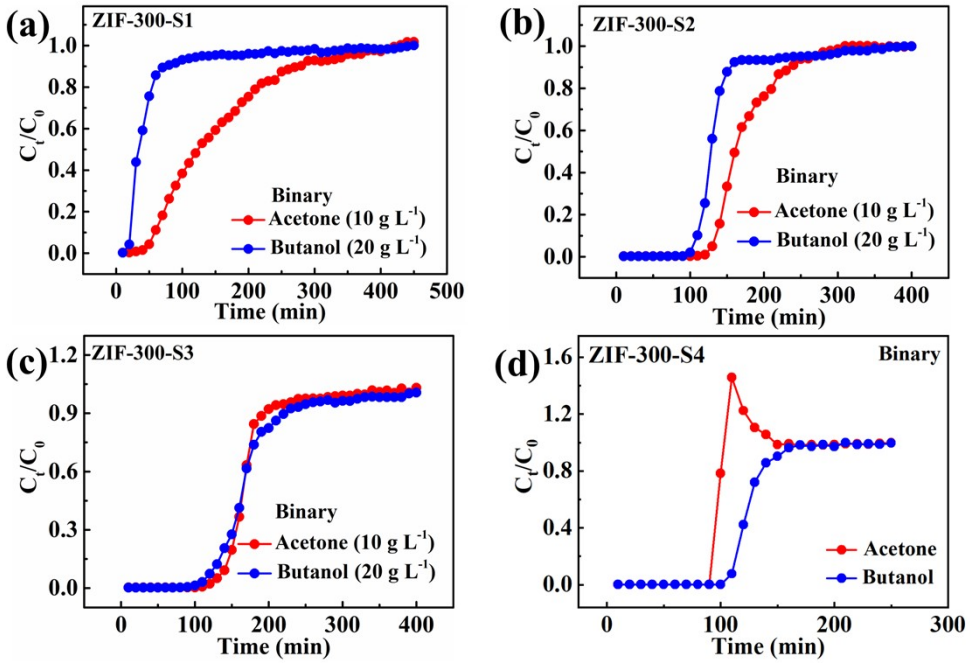

Figure S10 The breakthrough curves of the binary component aqueous solution (acetone/butanol: 10.0/20.0 g L^{-1}) of (a) ZIF-300-S1, (b) ZIF-300-S2, (c) ZIF-300-S3, and (d) ZIF-300-S4 (packed column length: 25.0 cm; diameter: 0.4 cm; flow rate: 0.05 mL min^{-1}; temperature: 298 K)

Table S5 Summary of capacity and selectivity of breakthrough curves of acetone/butanol on ZIF-300-S1-S4 samples

Adsorbent	Adsorbate	Dynamic column adsorption of AB binary components	
		Adsorption Amount (mg g^{-1})	Acetone/Butanol selectivity
ZIF-300-S1	Acetone	42.5	2.9
	Butanol	28.3	
ZIF-300-S2	Acetone	46.0	1.4
	Butanol	76.6	
ZIF-300-S3	Acetone	50.9	0.98
	Butanol	101.2	
ZIF-300-S4	Acetone	50.7	0.8
	Butanol	127.2	

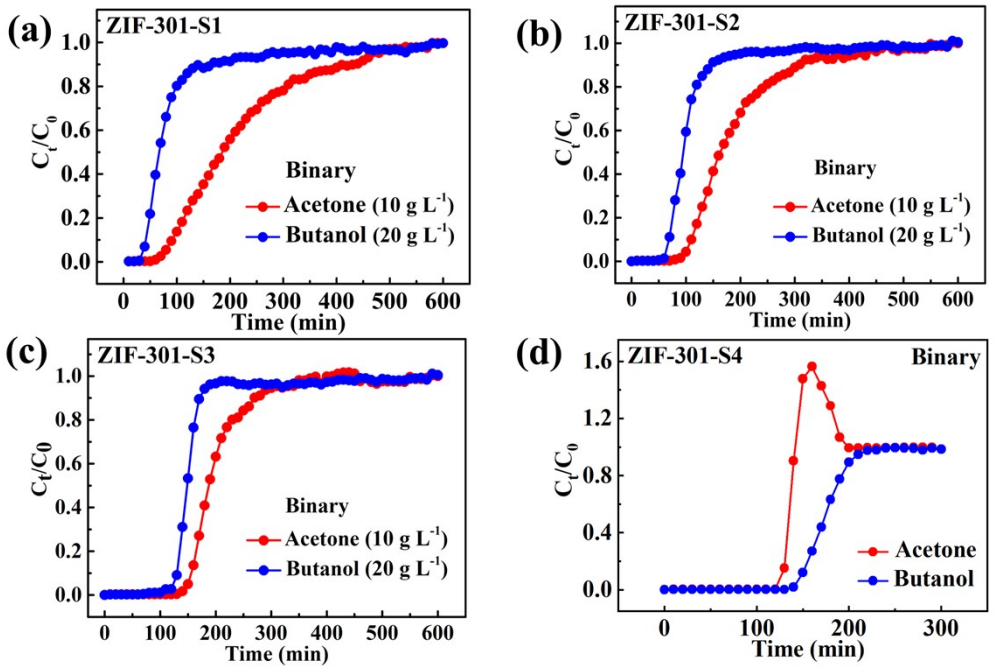

Figure S11 The permeation curves of the binary component aqueous solution (acetone/butanol: 10.0/20.0 g L^{-1}) of (a) ZIF-301-S1, (b) ZIF-301-S2, (c) ZIF-301-S3, and (d) ZIF-301-S4 (packed column length: 25.0 cm; diameter: 0.4 cm; flow rate: 0.05 mL min^{-1}; temperature: 298 K)

Table S6 Summary of capacity and selectivity of breakthrough curves of acetone/butanol on ZIF-301-S1-S4 samples

Adsorbent	Adsorbate	Dynamic column adsorption of AB binary components	
		Adsorption Amount (mg g^{-1})	Acetone/Butanol selectivity
ZIF-301-S1	Acetone	58.6	2.6
	Butanol	44.7	
ZIF-301-S2	Acetone	65.6	1.8
	Butanol	73.0	
ZIF-301-S3	Acetone	67.9	1.3
	Butanol	100.6	
ZIF-301-S4	Acetone	68.1	0.7
	Butanol	167.1	

Section S7: General rate model for breakthrough curves.

The breakthrough curve was fitted to the General Rate Model (GRM) with the following formulas: mass balance in the liquid phase (Equation S1) and in the solid phase (Equation S2), initial conditions (Equation S3) and boundary conditions (Equations S4–S6):

$$\frac{\partial c_i}{\partial t}+\frac{u}{\varepsilon_b}\frac{\partial c_i}{\partial x}+\frac{1-\varepsilon_b}{\varepsilon_b}\frac{3}{r_p}k_{film,i}\left[c_i-c_{p,i}(r=r_p)\right]=D_{ax}\frac{\partial^2 c_i}{\partial x^2} \quad (S1)$$

$$\varepsilon_p\frac{\partial c_{p,i}}{\partial t}+(1-\varepsilon_p)\frac{\partial q_i}{\partial t}=\frac{1}{r^2}\frac{\partial}{\partial r}\left[r^2\left(\varepsilon_p D_{pore,i}\frac{\partial c_{p,i}}{\partial r}\right)\right] \quad (S2)$$

$$t=0;\ c_i(0,x)=0;\ c_{p,i}(0,x,r)=0;\ q_i(0,x,r)=0 \quad (S3)$$

$$x=0:\ D_{ax}\frac{\partial c_i(t,0)}{\partial x}=\frac{u}{\varepsilon_b}(c_i(t,0)-c_0);\ x=L:\ \frac{\partial c_i(t,L)}{\partial x}=0 \quad (S4)$$

$$r=r_p:\ k_{film,i}\left[c_i-c_{p,i}(t,x,r_p)\right]=\varepsilon_p D_{pore,i}\frac{\partial c_{p,i}(t,x,r)}{\partial r} \quad (S5)$$

$$r=0:\ \frac{\partial c_{p,i}(t,x,0)}{\partial r}=0;\ \frac{\partial q_i(t,x,0)}{\partial r}=0 \quad (S6)$$

Among them, c_i, $c_{p,i}$, q_i represent the concentration of the adsorbate, the concentration of the adsorbate in the ZIF particles, and the amount of ZIFs' adsorption, respectively; i represents the type of adsorbate, D_{ax} is the axial diffusion coefficient, $k_{film,i}$ is the film mass transfer coefficient, $D_{pore,i}$ is the pore diffusion coefficient, u is the superficial velocity of the concentration of the adsorbate, x is the axial position, t is the time, ε_b is the bed void fraction, ε_p is the pore porosity, r is the particle radial distance and r_p is the particle radius.

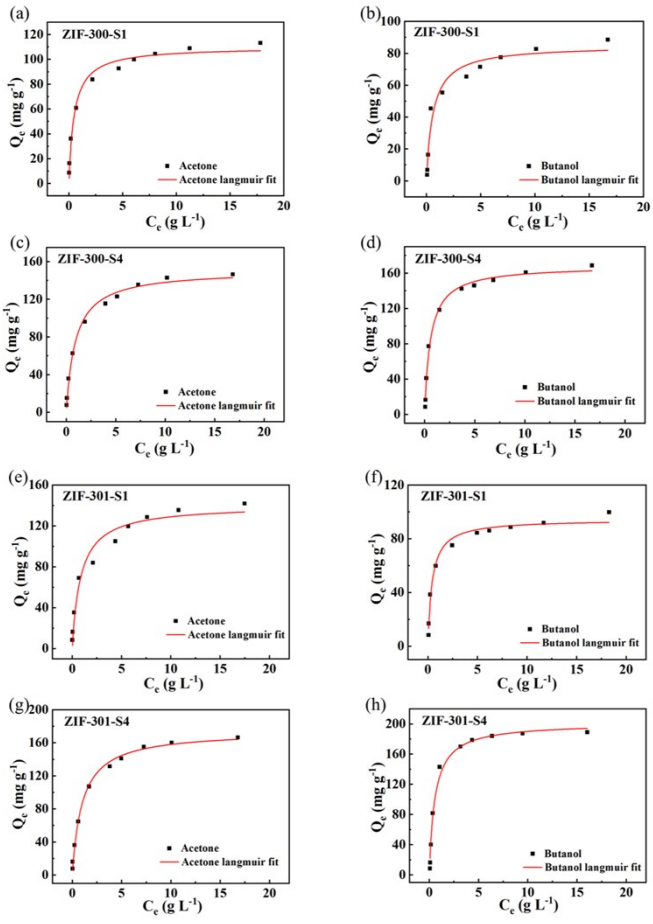

Figure S12 The Langmuir fitting for single component acetone and butanol static adsorption isotherm of ZIF-300 and ZIF-301 derivatives

Table S7 Summary of Langmuir fitting parameters for single component acetone and butanol static adsorption isotherm of ZIF-300 and ZIF-301 derivatives

Adsorbents	Adsorbates	Langmuir fit (y=a*x/(1+b*x))		
		a	b	R^2
ZIF-300-S1	Acetone	217.0±30.8	2.0±0.3	0.9832
	Butanol	135. 074±28.0	1.6±0.4	0.9622
ZIF-300-S4	Acetone	160.7±16.6	1.1±0.1	0.9907
	Butanol	287.5±27.3	1.7±0.2	0.9915
ZIF-301-S1	Acetone	159.3±33.8	1.1±0.3	0.9638
	Butanol	220.0±29.7	2.3±0.3	0.9811
ZIF-301-S4	Acetone	170.2±13.6	1.0±0.1	0.9944
	Butanol	345.7±40.2	1.7±0.2	0.9860

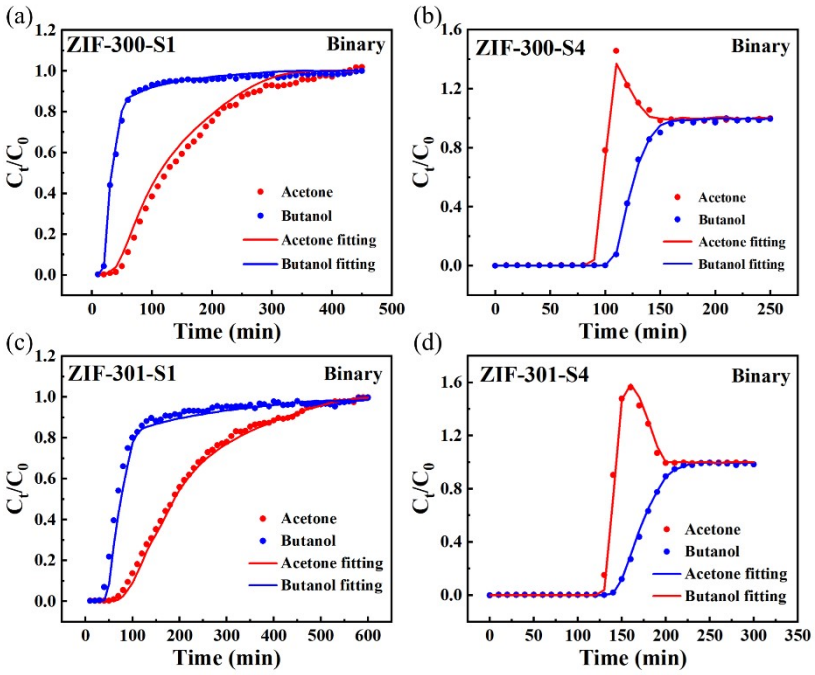

Figure S13 Breakthrough curves of binary-component (acetone: 10.0 g L^{-1}, butanol: 20.0 g L^{-1}) in dilute aqueous solutions at 25 °C: (a) ZIF-300-S1, (b) ZIF-300-S4, (c) ZIF-301-S1 and (d) ZIF-301-S4. The binary-component breakthrough curves were calculated by GRM model.

The simulated breakthrough curves by the GRM for adsorption of binary components onto ZIFs were in close agreement with the experimental results (Figure S13 and Table S8). For butanol adsorption, wider breakthrough profiles were observed on ZIF-300-S1 and ZIF-301-S1, while the profiles on ZIF-300-S4 and ZIF-301-S4 became much sharper. The pore diffusion coefficient of butanol increased significantly with the increase in pore aperture of ZIFs. For acetone adsorption, a significant broadening of the breakthrough profiles was observed on ZIF-300-S1 and ZIF-301-S1, and a sharp breakthrough profile was obtained on ZIF-300-S4 and ZIF-301-S4. The pore diffusion coefficient of acetone on ZIF-300-S1 and ZIF-301-S1 was one order of magnitude smaller than that of ZIF-300-S4 and ZIF-301-S4. Thus, the diffusion of acetone in the pore aperture of ZIF-300-S1 and ZIF-301-S1 may be limited.

Table S8 GRM simulated model parameters of binary-component breakthrough curves

Adsorbents	Adsorbates	GR model parameters		
		k_{film}	D_{ax}	D_{pore}
ZIF-300-S1	Acetone	1.01	1.90×10^{-4}	7.47×10^{-6}
	Butanol	1.03	4.15×10^{-4}	1.50×10^{-5}
ZIF-300-S4	Acetone	1.02	1.21×10^{-4}	3.16×10^{-5}
	Butanol	1.05	1.11×10^{-4}	2.10×10^{-5}
ZIF-301-S1	Acetone	1.01	1.25×10^{-4}	7.21×10^{-6}
	Butanol	1.03	3.22×10^{-4}	1.33×10^{-5}
ZIF-301-S4	Acetone	1.02	1.16×10^{-4}	4.21×10^{-5}
	Butanol	1.05	1.00×10^{-4}	2.31×10^{-5}

Section S8: Summary of cycling stability of ZIF-300 and ZIF-301 derivatives.

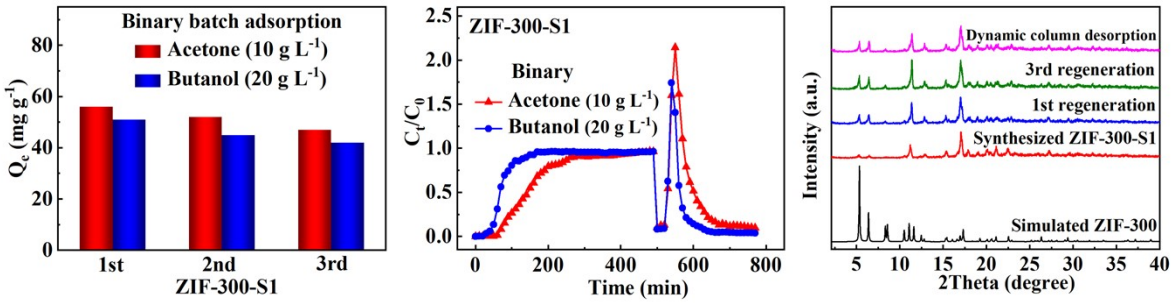

Figure S14 (a) Static cycle adsorption capacity, (b) dynamic column ads-desorption curves and (c) PXRD of ZIF-300-S1

Table S9 Summary of dynamic column adsorption and desorption capacities, and desorption rate of ZIF-300-S1 and ZIF-301-S1 for binary components (acetone/butanol: 10.0/20.0 g L^{-1})

Adsorbent	Adsorbate	Dynamic column adsorption and desorption of acetone/butanol binary components		
		$Q_{ads,i}$ (mg g^{-1})	$Q_{des,i}$ (mg g^{-1})	D_i (%)
ZIF-300-S1	Acetone/Butanol	45.7/33.8	38.2/27.4	83.4/81.2
ZIF-301-S1	Acetone/Butanol	58.7/44.7	47.5/36.3	81.0/81.2

Section S9: The schematic diagram and photos of the breakthrough device.

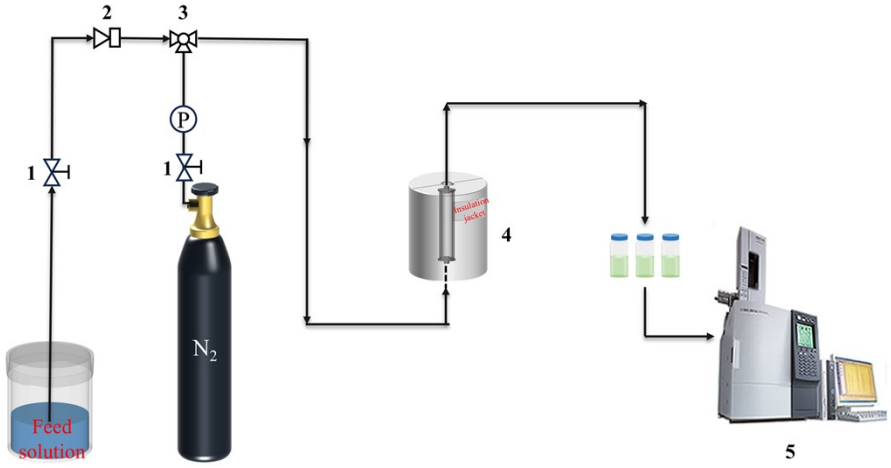

1.Two-way valve 2.Syringe pump 3.Three-way valve 4.Adsorption column and insulation device 5.Gas chromatograph (GC)

Figure S15 The schematic diagram of the breakthrough device

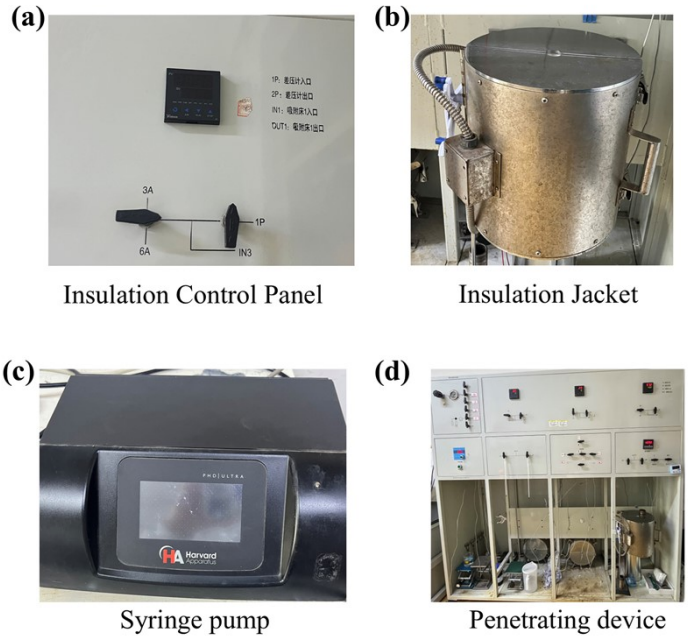

Figure S16 Partial assembly diagram of penetration device

Section S10: The computation of isosteric heat in Materials Studio.

The isosteric heat was derived using the Clausius-Clapeyron equation, based on the interaction energy between the adsorbate molecules and the ZIF framework, obtained from grand canonical Monte Carlo (GCMC) simulations in Materials Studio 2023. The calculations were performed using the Sorption Calculation module under fixed pressure conditions with the Metropolis method. The relevant formulas are as follows:

Isosteric heat and grand potential：The isosteric heat, Q, of a component is defined as the partial molar enthalpy of the sorbate component in the reservoir minus that in the framework:

$$Q^{SF} = h^S - h^F \tag{1-1}$$

Since the framework is typically favored over the gaseous reservoir, the value of the isosteric heat is usually positive. At equilibrium:

$$h^S - h^F = T(s^S - s^F) \tag{1-2}$$

where s is the partial molar entropy. So, using the Clapeyron equation, the following expression is obtained:

$$Q^{SF} = (v^S - v^F)\left[\frac{dp}{d(lnT)}\right] = RT\left[\frac{d(lnp)}{d(lnT)}\right] \tag{1-3}$$

In the second expression, the partial molar volume in the framework is neglected with respect to that in the reservoir and the reservoir is assumed to be ideal. The remaining partial derivative can be evaluated in the grand canonical ensemble, leading to:

$$Q^{SF} = RT - G \tag{1-4}$$

where G is defined as:

$$G = \langle E \rangle - \mu_{intra}\langle N \rangle \tag{1-5}$$

In Sorption, G is referred to as the"grand potential". If the lowest energy configurations are returned, they are ordered by the value of the grand potential.